



1 **Intensive agricultural management-induced**
2 **subsurface accumulation of water extractable**
3 **colloidal P in lime concretion black soil**

4 Shouhao Li^{a,b}, Shuiqing Chen^a, Shanshan Bai^a, Jinfang Tan^{a,b*}, Xiaoqian Jiang^{a,b*}

5 ^a School of Agriculture, Sun Yat-sen University, Guangzhou, Guangdong 510275, PR
6 China

7 ^b Modern Agricultural Innovation Center, Henan Institute of Sun Yat-sen University, PR
8 China

9 Corresponding to: jiangxq7@mail.sysu.edu.cn and tanjf7@mail.sysu.edu.cn

10

11 **ABSTRACT:**

12 Long-term excessive application of mineral fertilizer leads to accumulation of
13 phosphorus (P) in lime concretion black soil, which increases the risk of P migration
14 and loss from soil profile. The colloids in the profile are important carriers for P
15 migration due to high P adsorption and transport capacity. In this study, water
16 extractable colloids (WECs) were obtained from 0 ~ 120 cm soil profile by soil
17 fractionation method, and their physicochemical properties were analyzed. Solution ³¹P
18 nuclear magnetic resonance (NMR) and P K-edge XANES were used to characterize
19 the species and distribution of colloidal P in fertilized farmland soil profile. Total and
20 available P in bulk soil and colloids decreased with soil depth. The organic P (OP)
21 contained ~97 to 344 mg kg⁻¹ per bulk soil and 110-630 mg/kg per WECs in soil profile
22 with composition of orthophosphate monoesters and diesters according to NMR results.
23 It suggested that OP in WECs from subsoils might be affected by the translocation of
24 colloidal P (CP) from surface soils probably due to soil acidification and preferential
25 flow caused by swelling-shrinkage clays including montmorillonite and nontronite.
26 Additionally, the more negative zeta potential of surface soil colloids suggests the high
27 mobility of colloidal P to the subsoils. The CP concentrations for <2 μm was about 38-



28 93 mg/kg per bulk soil, which is 6-37 folds of dissolved reactive P (DRP)
29 concentrations, suggesting that the role of CP for P transport in the soil profile is
30 dominated. This study showed that inorganic and organic P migrated from surface to
31 deeper layer along the lime concretion black soil profile, with soil colloids having a
32 significant effect on P migration from both surface and subsurface layers. The results
33 have an important significance for soil P migration evaluation and agricultural non-
34 point source pollution control in lime concretion black soil.

35 **Keywords:** Subsurface soil; Water extractable colloids, Organic P, Solution 31P-NMR,
36 P K-edge XANES

37 **INTRODUCTION:**

38 Phosphorus (P) as one of essential macronutrients for crops is strongly immobilized
39 with inorganic and organic soil components (Arai and Sparks, 2007). The lime
40 concretion black soil is characterized by low water-air permeability, poor fertility, and
41 strong swelling-shrinkage properties (Chen *et al.*, 2020). Therefore, high-intensity
42 agriculture practices such as excessive fertilization have been applied for decades to
43 maintain grain yields. Additionally, artificial ditches (~1-1.5 m depth) are usually dug
44 out in the edge of field to facilitate drainage. However, long-term excessive input of
45 mineral fertilizers may result in considerable P accumulation in agricultural soils and
46 the artificial ditches bring increasing risk of P losses into surface water and ground
47 water, causing serious environmental issues such as outbreaks of cyanobacteria and
48 eutrophication (Whalen and Chang, 2001; Koopmans *et al.*, 2003; Hansen *et al.*, 2004).
49 In addition to the transport of soil surface P (Pote *et al.*, 1996), transport of soil
50 subsurface P has also been considered as a crucial pathway to waterways (Jorgensen
51 and Fredericia, 1992; Kronvang *et al.*, 1997; Xue *et al.*, 1998; Hens and Merckx, 2001;
52 Williams *et al.*, 2016; Jiang *et al.*, 2021). Some researchers have reported that high
53 rainfall events promote the losses of P from tile drainage (1.0-1.4 m depth) (Royer *et al.*,
54 2006). In previous study in USA, colloidal P was the dominant P fraction of total P
55 in tile water during high rainfall events (Jiang *et al.*, 2021). The colloids were found to
56 carry over 1000 mg of P kg⁻¹, which was dominated in the transported P from subsurface



57 soil (Jiang *et al.*, 2021).

58 Currently, only a few papers have investigated dissolved and colloidal P distribution in
59 subsoils which involved forest soils and Mollisols (Gentry *et al.*, 2007; Wang *et al.*,
60 2020; Li *et al.*, 2022). However, it is still not clear about the distribution of mobile
61 colloidal P as well as their speciation in the soil profile of lime concretion black soil.
62 Furthermore, whether the transport of colloidal P from topsoils to subsoils occurs and
63 contributes to total P in subsurface flow is not clearly understood. Considering that the
64 presence of shrink and swell clays in lime concretion black soil, the translocation of
65 dissolved and colloidal P from surface soil to subsoils by preferential flow is expected
66 as an important P transport pathway and leads to spatial redistribution within soil
67 profiles. Additionally, the artificial ditches could also facilitate the transport of
68 dissolved and colloidal P from both surface and subsurface soil, which is an important
69 non-point source of eutrophication. Furthermore, the intensive input of fertilizer in lime
70 concretion black soil (~600 kg/hm² compound fertilizer, N-P-K: 28-6-6) was also
71 expected to facilitate the release of colloidal P (Liang *et al.*, 2016).

72 It is accepted that colloidal P could be derived from surface soils if the mobile colloids
73 in subsurface soil contains organic P (Li *et al.*, 2022). The aim of this research was to
74 explore (1) the dispersion of water-extractable colloids (WECs) in the soil profile for
75 intensively managed lime concretions black soil and (2) physicochemical properties
76 and P speciation of WECs with different depths. This information is the first for the
77 assessment of colloidal P release potential from subsoils in lime concretion black soil
78 and is valuable for the construction of sustainable strategies to control agricultural P
79 loss.

80 **2. MATERIALS AND METHODS**

81 **2.1 Site description and soil sampling**

82 The selected site was located at the agricultural study site in Pingyu County, Henan
83 Provinces, China with precipitation of 904.3 mm and annual mean temperature of 15 °C,
84 respectively. According to the World Reference Base for soil resources (WRB, 2014),
85 the soil type found in this region is lime concretion black soil. Soil samples defined as



86 A, B, C, and D were collected from four sites: Chenji Village (33°00'N and 114°51'E),
87 Dingying Village (33°09'N and 114°49'E), Xinggang Village (32°99'N and 114°84'E),
88 and Hanqiao Village (32°56'N and 114°49'E). Samples were taken along four vertical
89 profiles at five or six different depths, i.e., 0-20, 20-40, 40-60, 60-80, 8-120 cm (or 80-
90 100 and 100-120 cm), which are denoted as depth 1, 2, 3, 4, 5 (or 5 and 6), respectively.
91 The cultivation system in the region involved rotating winter wheat and summer maize
92 crops. The fertilizers for winter wheat contained 750 kg/hm² compound fertilizer (N-P-
93 K: 15-15-15) and 300 kg/hm² urea. Those for summer maize included 600 kg/hm²
94 compound fertilizer and 225 kg/hm² urea. The samples were air-dried, ground, and
95 passed through 2-mm sieve before analysis.

96 **2.2 Physicochemical characterization of the soils**

97 Soil pH was assessed by using a pH meter with a soil-to-water ratio of 1:2.5. Soil total
98 carbon (C) and nitrogen (N) levels were analyzed with an elemental analyzer (Jin *et al.*,
99 2016). Oxalate extracted P (i.e. OA-P) was extracted by ammonium oxalate and oxalic
100 acid (Jiang *et al.*, 2015) and considered as the P bonded to amorphous, poorly crystalline
101 and organo-Fe/Al (hydr)oxides (Masiello *et al.*, 2004; Kleber *et al.*, 2005; Neubauer *et*
102 *al.*, 2013). The dithionite-citrate-bicarbonate (i.e. DCB) extracted P was extracted by
103 sodium citrate solution, sodium hydrogen carbonate solution and sodium dithionite
104 (Jiang *et al.*, 2015) and considered as P associated with organically bound, amorphous
105 and crystalline Fe oxides. The activities of acid and alkaline phosphatase, denoted as
106 ACP and ALP respectively, were determined by performing *p*-nitrophenyl phosphate
107 assays on moist soil samples at two pH conditions, 6.5 and 11 respectively (Tabatabai
108 *et al.*, 1969). Soil available P was extracted with 0.5 M NaHCO₃ at pH 8.5 (Van Lierop,
109 1988) and measured by molybdate blue colorimetry (Murphy and Riley, 1962). Total
110 inorganic P (TIP) was extracted by sulfuric acid and dilute sodium hydroxide solution
111 separately via the sequential extraction method by Kronvang *et al.*(1997) and measured
112 by molybdate blue colorimetry. For the total P (TP), the extracts that were acquired
113 from the acid and base treatments were treated with potassium persulfate and sulfuric



114 acid before molybdate blue colorimetry and the sum of digested extracts was defined
115 as TP. The total organic P (TOP) was the difference between TP and TIP.

116 **2.3 Soil particle separations and characterization of water extractable** 117 **colloids**

118 The soil samples of A and B with different depths were fractionated by the method
119 described by Séquaris et al. (2003). Briefly, 100 g of soil was dispersed in 200 mL Milli-
120 Q water in a 1 L Duren bottle and shaken for 6 h at 150 rpm. Then 600 mL Milli-Q
121 water was added and mixed to settle. The particles $>20\ \mu\text{m}$ and $2\text{-}20\ \mu\text{m}$ were obtained
122 by removing the supernatant after settling for 6 min and 12 h, respectively. The
123 supernatant was subsequently spun at $3500\times g$ for 5 min to obtain the water extractable
124 colloids with size of $0.35\text{-}2\ \mu\text{m}$ (calculated based on Stokes' law). The final supernatant
125 is defined as “dissolved fraction” although a small quantity of nanoparticles might be
126 present. The dissolved reactive P (DRP) and dissolved total P (DTP) were measured by
127 molybdate blue colorimetry (Murphy and Riley, 1962) before and after the digestion of
128 potassium persulfate and sulfuric acid for the “dissolved fraction”.

129 To elucidate the inorganic and organic P species, the extracted colloidal samples from
130 sample A and B with different depths were selected for the NMR analysis. The colloid
131 samples (1 g) were mixed with 10 mL of solution containing 0.25 M NaOH and 0.05
132 M Na_2EDTA for 4 h (Jiang *et al.*, 2017). After that, extracts were centrifuged at 10000
133 $\times g$ for 30 minutes. The P, Fe, and Mn contents in the supernatant were measured by
134 inductively coupled plasma optical emission spectroscopy (ICP-OES). The rest
135 supernatant was freeze-dried and then 100 mg freeze-dried extracts were dissolved in
136 0.1 mL D_2O and 0.9 mL of a solution containing 1.0 M NaOH and 0.1 M Na_2EDTA .
137 After being prepared, the samples underwent centrifugation for 20 minutes at $10000\times g$.
138 The resulting supernatant was subsequently analyzed using a Bruker 500-MHz
139 spectrometer with a 5 mm NMR tube. The NMR parameters contained 0.68 s
140 acquisition time, 90° pulse width, 8000 scans, and proton decoupling. The relaxation
141 time, which fell within the range of 3-6 seconds, was estimated by correlating



142 P/(Mn+Fe) with spin-lattice relaxation times (McDowell *et al.*, 2006). The spiking
143 samples with myo-inositol hexakisphosphate (myo-IHP), α - and β - glycerophosphate,
144 and adenosine monophosphate were cited to facilitate peak identification (Bai *et al.*,
145 2023). The α -, β -glycerophosphates and mononucleotides (Glyc+nucl) were classified
146 as orthophosphate diesters rather than to monoesters (Young *et al.*, 2013; Liu *et al.*,
147 2018). The area under each peak was determined by integrating spectra that were
148 processed with a line broadening of 2 and 7 Hz. Mestrenova 10.0.2 software was used
149 to process all spectra. Additionally, zeta potential of colloids from sample A and B with
150 different depths were measured using a Zetasizer (Malvern). The X-ray powder
151 diffractometer (XRD, Empyrean) was selected to identify mineral compositions for soil
152 colloids in the 2θ range from 3° to 90° with the scan step size of 0.026° and the scan
153 rate of $10^\circ \text{ min}^{-1}$.

154 To elucidate the P bonding fractions in the WEC fractions, the P K-edge X-ray
155 absorptions near-edge structure (XANES) measurements were performed at Beamline
156 4B7A of the Beijing Synchrotron Radiation Facility, Beijing, China. The following
157 standard samples were chosen: aluminum phosphate (Al-P, AlPO_4), iron phosphate
158 dihydrate (Fe-P, $\text{FePO}_4 \cdot 2\text{H}_2\text{O}$), inositol hexakisphosphate (IHP), and hydroxyapatite
159 (HAP, $\text{Ca}_5(\text{PO}_4)_3\text{OH}$). The soil spectra were collected using a SiLi detector in PFY
160 mode, providing detailed information about the fluorescence yield. The spectra of P
161 standard samples were measured in total electron mode without self-absorption.
162 Multiple spectra (three repetitions for soil samples) were collected and averaged. All
163 XANES spectra were measured by Athena (0.9.26). The absolute energy scale was
164 calibrated to 2149 eV (E_0) as the maximum energy of the first peak in the first
165 derivative spectrum of AlPO_4 (Beauchemin *et al.*, 2003). Linear combination fitting
166 (LCF) of the soil P spectra was conducted in the relative energy range between -10 and
167 30 eV. The goodness of fit was judged by the chi-squared values and R values, and P
168 standard samples yielding the best fit were considered as the most possible P species in
169 the investigated soil samples.

170 **2.4 Statistical analysis**



171 One way ANOVA and single factor analysis of variance were used to test significant
172 differences of soil indicators with different soil profiles. Tukey's honesty significance
173 difference (HSD) test was used, and the significance level was 0.05. SPSS 25.0 and
174 Excel software were used for statistical analysis. These data were created using
175 OriginPro 2021 (OriginLab Corp., Northampton, MA, USA).

176 **3. RESULTS AND DISCUSSION**

177 **3.1 Physicochemical characterization and P distribution of Soil profile**

178 As the depth increased in all soil samples, the soil pH exhibited a significant overall
179 increase from acidic to alkaline conditions, ranging from 4.88 to 8.37 (Table 1). The
180 serious acidity of the topsoil (0-20 cm) is probably due to increasing release of protons
181 by nitrification processes after excessive application of nitrogen fertilizers (750 kg/hm²
182 compound fertilizer and 300 kg/hm² urea per year in the studied area) and the
183 continuous removal of base cations by crop harvest (Guo *et al.*, 2010). The calcareous
184 nature of lime concretion black soil at the study site contributed to subsoils with pH
185 values of slight alkalinity. The contents of total carbon (from 1.17 to 0.25%) and total
186 nitrogen (from 0.14 to 0.03%) decreased significantly from topsoil to subsoil (Table 1).
187 The accumulation of total C and N in surface soil (0-20 cm) could be related to the
188 increased organic matter contents by biomass inputs from crop residue and N
189 fertilization. The deepest layer soil (80-120 cm) contained the highest pH values and
190 lowest total C and N contents, suggesting that the subsurface soil (20-80 cm) was also
191 influenced by these intensive agricultural managements to some extent. The activities
192 of acid phosphatase (ACP) was as high as 1177 µg/(g*h) in topsoil and decreased with
193 the depth of soil layer as low as 96.2 µg/(g*h) in subsoil (Table 1). The activities of
194 both acid and alkaline (ALP) phosphatase decreased significantly with depth for all the
195 samples. The ACP was higher in the surface soil (0-20 cm) but was lower in the
196 subsurface soil (20-120 cm) compared to ALP. Acid phosphatase activity, mainly
197 released by plant roots and fungi, is predominant in acidic soils (Eivazi *et al.*, 1977;
198 Juma and Tabatabai, 1977; Arenberg *et al.*, 2020). Alkaline phosphatase activity,
199 primarily produced by soil microbes, is optimized in neutral and alkaline conditions



200 (Juma and Tabatabai, 1988; Dick *et al.*, 2000; Krämer and Green, 2000). The higher
201 acid phosphatase activity in surface soil may be attributed to acidic pH and the
202 rhizosphere effect, where plant roots and fungi are easily concentrated (Häussling *et al.*,
203 1989). Thus, lower acid phosphatase activity in the subsurface soil (< 20 cm) was due
204 to increasing pH with depth.

205 Oxalate extractable P concentration ranged from ~30-162 mg kg⁻¹ (~7-45% of TP) in
206 all soils (Table 1). The oxalate extractable P concentration in the surface soils was ~127
207 to 162 mg/kg and it accounted for 19-27% of TP and ~76 to 98 % of DCB extractable
208 P, suggesting that amorphous Fe/Al oxides bounded P was dominated for the Fe-P in
209 the surface soils compared to crystalline Fe/Al oxides. Many studies have reported that
210 the majority of P was associated with amorphous Fe /Al oxides fractions in many soil
211 types (Rick and Arai, 2011; Jiang *et al.*, 2015). It has been reported that specific anion
212 adsorption such as P suppressed the transformation of amorphous Fe oxides to
213 crystalline Fe oxides (Biber *et al.*, 1994), supporting the lower amount of P associated
214 with crystalline Fe oxides.

215 The concentrations for TIP, TOP, and TP are included in Fig.1. The total P
216 concentrations in all soil samples were observed to range from approximately 230 to
217 670 mg kg⁻¹, and exhibited a generally decreasing trend with increasing soil depth. (Fig.
218 1). Total inorganic P accounted for ~48 to 65% of TP and TOP accounted for ~35 to 52%
219 of TP in all soil samples. Organic P accumulation (~97 to 344 mg kg⁻¹) was measured
220 in all soil depths. The C/P ratio of > 200:1 is favorable for P immobilization (Dalal and
221 Hallsworth, 1977; Sanyal and De Datta, 1991). The C/P ratio of soil samples in this
222 study was about 9.5 to 22.1, which promoted P mineralization. Thus, the accumulation
223 of organic P in the surface soil would be due to the increasing organic matter contents,
224 rather than the biological immobilization of P. Gradual transport of OP from surface to
225 subsoils could contribute to the accumulation of OP in the subsoils. Available P was
226 very high with ~20 to 40 mg kg⁻¹ in the surface soils but decreased dramatically with
227 increasing depth in all samples (Fig. 1). The available P content in the topsoil has been
228 classified as "high", and a threshold of 20 mg/kg has been regarded as optimal growth



229 level for crops (Li *et al.*, 2015). This implies that the surface soils (0-20 cm) contained
230 enough available P for the growth of winter wheat and corn.

231 **3.2 Physicochemical properties of water extracted colloids (WECs)**

232 Considering that all four samples showed similar physicochemical properties and P
233 distribution, we further investigated the colloids of samples A and B with different
234 depth. It is crucial to mention that the WECs are colloids that are well-defined with size
235 of 0.35-2 μm operationally. The major soil series are sandy loam and loam, with the
236 colloidal mass of 5.3 to 8.3% (Table 2). The colloidal mass increased with depths for
237 both samples and previous researcher has reported a similar tendency for the recovery
238 rate of WECs in dark-colored Mollisols (Li *et al.*, 2022). Notably, no colloids existed in
239 the depth > 60 cm for sample B, suggesting that the generation of colloids from
240 weathered minerals in subsoils was limited. It suggested that the colloids in the
241 depth >60 cm for sample A originated from the transport of upper soil colloids.

242 The XRD results further verified it considering that the colloids of sample A and B with
243 all depths contained the same mineral composition (Fig. 3). The minerals in all the
244 colloids included montmorillonite, nontronite, and illite, indicating the existence of
245 swelling-shrinkage clays. These secondary minerals all have a significant adsorption
246 capacity for P (Gérard, 2016; Chen *et al.*, 2020). Values of zeta potential for WECs
247 were approximately -20 mV at the surface soil, but the values increased with depth
248 (Table 2). A higher P concentration in surface soils could facilitate P special adsorption
249 to minerals of WECs such as iron oxyhydroxide (e.g. hematite, goethite, and
250 ferrihydrite) and aluminosilicate minerals (Arai and Sparks, 2001; Celi *et al.*, 2001;
251 Jiang *et al.*, 2015), causing the surface charge lower compared to that of WECs in
252 subsurface soils. The more negative values of zeta potential at surface soil suggests the
253 higher mobility of colloidal P from the surface soil to the subsoils. It is important to
254 note that DRP accounted for only 29-51% of DTP (Table 2). Furthermore, the sum of
255 colloidal P concentration for <0.35 μm (i.e. the difference between DTP and DRP) and
256 0.35-2 μm was about 38-93 mg/kg soil, which is 6-37 folds of DRP. It suggested that
257 the contribution of CP to transport P in both surface and subsurface soil environment is



258 important and should not be overlooked.

259 **3.3 Inorganic and organic P distribution in WECs with soil depth**

260 At each sampling site, the concentration of TP in WECs was found to be the highest in
261 the topsoil layer (0-20 cm), with a range of 1150 to 1300 mg kg⁻¹. (Fig. 3). The amounts
262 were significantly higher than the TP in bulk soils (~600-700 mg kg⁻¹). The soil colloids
263 enriched in secondary clays such as montmorillonite, nontronite, and illite as shown in
264 XRD results could readily immobilize P. Generally, the TP of colloids at each site was
265 found to decrease with increasing soil depth. Most colloidal P at the surface soil was
266 from fertilizers and plant residues. The concentration of total IP in WECs was found to
267 be high (ranging from 680 to 730 mg kg⁻¹) in the topsoil and displayed a decreasing
268 trend with increasing soil depth across all sites. As predicted, total OP concentration
269 was high (430-630 mg kg⁻¹) in the colloids of surface soil. This is associated with the
270 high OC concentration in the surface soil, and P was probably immobilized in the
271 organic matter of soil. The decline in tendency of OP concentrations with soil depth
272 was probably due to the decreasing OM contents. It is noteworthy that OP was still
273 presented in the WECs of subsoils where the C/P is less than 300 that could not support
274 immobilization for the accumulation of OP (Table 1 and 3). This finding implies that
275 colloidal-bound OP has the potential to be transported from topsoil to subsoil layers.

276 **3.4 Solution ³¹P NMR analysis and P K-edge XANES analysis**

277 The ³¹P NMR spectroscopy spectra of WECs were presented in Table 3. It is worth
278 mentioning that NaOH-EDTA extracted P in the NMR analysis was below 100 %.
279 Therefore, the concentrations of OP and IP did not correspond with the chemical
280 digestion data presented in Fig. 2. For inorganic P, orthophosphate was found in all
281 samples but pyrophosphate was only found in the surface soil. Pyrophosphate was
282 present in live fungal tissue and was easily decomposed (Koukol *et al.*, 2008). In
283 addition to inorganic P, the OP in the WECs of all depths for sample A and B contained
284 similar species including orthophosphate monoesters (36-128 mg kg⁻¹) and diesters (0-
285 89 mg kg⁻¹) according to NMR results (Table 3). It was clear that OP existed in mobile
286 colloids for both surface and subsoils, suggesting that OP in WECs from subsoils was



287 affected by the translocation of CP from surface soils (Li *et al.*, 2022). Colloids
288 containing clay minerals in the soil profile could retain orthophosphate monoesters and
289 diesters. Inositol phosphate has also been found to be adsorbed on amorphous metal
290 oxides and clay minerals (e.g. montmorillonite, illite, and kaolinite) (Barka and
291 Anderson, 1962; Celi *et al.*, 1999).

292 The normalized XANES spectra of WECs in sample A and B with soil profile are shown
293 in Table 4 and Fig. 4. Aluminum phosphate (Al-P), iron phosphate dihydrate (Fe-P),
294 hydroxyapatite (HAP), and inositol hexakisphosphate (IHP) were detected in WECs for
295 all the samples. The XANES results of WECs showed that the proportions of Al-P, Fe-
296 P, and IHP of WECs decreased but HAP increased with soil depth. As a typical alkaline
297 soil containing carbonate concretions, the lime concretions black soil facilitated the
298 formation of Ca-P minerals, thus causing low P availability for crops (Westermann,
299 1992; Iyamuremye *et al.*, 1996; Li *et al.*, 2011). The decrease of soil pH in the surface
300 soils accelerated the dissolution of Ca mineral phases, the release of associated colloidal
301 P, and the transformation of Ca-P to Al-P and Fe-P, thus increasing the concentrations
302 and proportions of higher activity inorganic P fractions (Zhao *et al.*, 2019). The
303 proportions of IHP decreased with soil depth but IHP still existed as certain amounts in
304 the subsoil, which further confirmed the results of NMR.

305 **4. CONCLUSIONS**

306 In this study, the distribution of WECs with soil profiles (0-120 cm) was investigated
307 in lime concretion black soil with high intensity agricultural management. The P-rich
308 WECs (0.35-2 μm) was dispersed from surface soils to subsoils with the proportion of
309 5.3-8.3% of bulk soil. The TP concentration in the WECs was as high as 1150-1300 mg
310 kg^{-1} . It is noteworthy that OP associated with WECs were found in subsurface soils,
311 indicating the colloidal P was transported from surface soils to subsoils, resulting in the
312 distribution of P-rich WECs throughout the entire soil profile. Soil colloids with a
313 greater negative charge resulting from P adsorption may be repulsed by negatively
314 charged soil mineral surfaces, leading to the transportation of these colloidal P to the
315 subsoil. The soil acidification in lime concretion black soil could facilitate deterioration



316 of Ca-stabilized aggregates, accelerated the release of associated colloidal P and
317 furthermore shifted the composition from Ca dominated colloids to Fe/Al oxides enrich
318 ones. The existence of swelling-shrinkage minerals such as montmorillonite and
319 nontronite promoted preferential flow and the transport of colloidal P. Furthermore, the
320 artificial ditches could also facilitate the transport of WECs from surface soil to subsoils.
321 The sum of colloidal P $< 2 \mu\text{m}$ was 6-37 folds of DRP, suggesting that the contribution
322 of CP to P transport in the whole soil profile is predominant. Thus, it is crucial to take
323 into account the impact of colloidal P when predicting P loss from surface to subsurface
324 flow.

325

326 **References:**

- 327 Arai, Yuji, and DL Sparks. "Phosphate Reaction Dynamics in Soils and Soil Components: A Multiscale
328 Approach." *ADVANCES IN AGRONOMY*, 94, 135-79. [https://doi.org/doi.org/10.1016/S0065-2113\(06\)94003-6](https://doi.org/doi.org/10.1016/S0065-2113(06)94003-6). 2007.
- 329
- 330 Arai, Yuji, and Donald L Sparks. "Atr-Ftir Spectroscopic Investigation on Phosphate Adsorption
331 Mechanisms at the Ferrihydrite-Water Interface." *JOURNAL OF COLLOID INTERFACE
332 SCIENCE* 241, no. 2 317-26. <http://doi.org/org10.1006/jcis.2001.7773>. 2021
- 333 Arenberg, Mary R, Xinqiang Liang, and Yuji Arai. "Immobilization of Agricultural Phosphorus in
334 Temperate Floodplain Soils of Illinois, USA." *BIOGENCHEMISTRY*, 150, no. 3, 257-78.
335 <https://doi.org/10.1007/s10533-020-00696-1>. 2020.
- 336 Beauchemin, Suzanne, Dean Hesterberg, Jeff Chou, Mario Beauchemin, Régis R Simard, and Dale E
337 Sayers. "Speciation of Phosphorus in Phosphorus-Enriched Agricultural Soils Using X-Ray Absorption
338 near-Edge Structure Spectroscopy and Chemical Fractionation." *JOURNAL OF ENVIRONMENTAL
339 QUALITY*, 32, 1809-19. <https://doi.org/10.2134/jeq2003.1809>. 2003.
- 340 Biber, Madeleine V, and Werner Stumm. "An in-Situ Atr-Ftir Study: The Surface Coordination of
341 Salicylic Acid on Aluminum and Iron (Iii) Oxides." *ENVIRONMENTAL SCIENCE TECHNOLOGY*, 28, 763-68. <https://doi.org/10.1021/es00054a004>. 1994.
- 342 Celi, L, M Presta, F Ajmore-Marsan, and Elisabetta Barberis. "Effects of Ph and Electrolytes on Inositol
343 Hexaphosphate Interaction with Goethite." *SOIL SCIENCE SOCIETY OF AMERICA
344 JOURNAL*, 65, 753-60. <https://doi.org/10.2136/sssaj2001.653753x>. 2001.
- 345
- 346 Chen, Lin, Fang Li, Wei Li, Qi Ning, Jingwang Li, Jiabao Zhang, Donghao Ma, and Congzhi Zhang.
347 "Organic Amendment Mitigates the Negative Impacts of Mineral Fertilization on Bacterial Communities
348 in Shajiang Black Soil." *APPLIED SOIL ECOLOGY*, 150, 103457.
349 <https://doi.org/10.1016/j.apsoil.2019.103457>. 2020.
- 350 Dalal, RC, and EG Hallsworth. "Measurement of Isotopic Exchangeable Soil Phosphorus and
351 Interrelationship among Parameters of Quantity, Intensity, and Capacity Factors." *SOIL SCIENCE
352 SOCIETY OF AMERICA JOURNAL* 41, 8186 <https://doi.org/10.2136/sssaj1977.03615995004100010025x>. 2003.
- 353
- 354 Dick, Warren A, L Cheng, and P Wang. "Soil Acid and Alkaline Phosphatase Activity as Ph Adjustment



- 355 Indicators."SOIL BIOLOGY BIOCHEMISTRY,32, 1915-19. [https://doi.org/10.1016/S0038-](https://doi.org/10.1016/S0038-0717(00)00166-8)
356 [0717\(00\)00166-8](https://doi.org/10.1016/S0038-0717(00)00166-8).2000.
- 357 Eivazi, F, and MA Tabatabai. "Phosphatases in Soils." SOIL BIOLOGY BIOCHEMISTRY 9, 167-72.
358 [https://doi.org/10.1016/0038-0717\(77\)90070-0](https://doi.org/10.1016/0038-0717(77)90070-0).1977.
- 359 Gérard, Frédéric "Clay Minerals, Iron/Aluminum Oxides, and Their Contribution to Phosphate
360 Sorption in Soils—a Myth Revisited."GEODERMA,262,213-26.
361 <https://doi.org/10.1016/j.geoderma.2015.08.036>.2016.
- 362 Guo, JH, XJ Liu, Yong Zhang, JL Shen, WX Han, WF Zhang, P Christie, et al. "Significant Acidification
363 in Major Chinese Croplands." SCIENCE,327, no. 5968,1008-10.
364 <https://doi.org/10.1016/j.scitotenv.2017.09.289>.2010.
- 365 Hansen, Jeremy C, Barbara J Cade-Menun, and Daniel G Strawn. "Phosphorus Speciation in Manure-
366 Amended Alkaline Soils." JOURNAL OF ENVIRONMENTAL QUALITY, 33, no. 4 ,1521-27.
367 <https://doi.org/10.2134/jeq2004.1521>.2004.
- 368 Häussling, M, and H Marschner. "Organic and Inorganic Soil Phosphates and Acid Phosphatase Activity
369 in the Rhizosphere of 80-Year-Old Norway Spruce [Picea Abies (L.) Karst.] Trees." BIOLOGY
370 FERTILITY OF SOILS, 8, no. 2 , 128-33. <https://doi.org/10.1007/bf00257756>.1989
- 371 Hens, Maarten, and Roel Merckx. "Functional Characterization of Colloidal Phosphorus Species in the
372 Soil Solution of Sandy Soils." ENVIRONMENTAL SCIENCE TECHNOLOGY, 35, no. 3 , 493-500.
373 <https://doi.org/10.1021/es0013576>.2001.
- 374 Iyamuremye, F, RP Dick, and J Baham. "Organic Amendments and Phosphorus Dynamics: II.
375 Distribution of Soil Phosphorus Fractions." SOIL SCIENCE, 161, no. 7, 436-43.
376 <https://doi.org/10.1097/00010694-199607000-00003>.1996
- 377 Jiang, Xiaoqian, Wulf Amelung, Barbara J Cade-Menun, Roland Bol, Sabine Willbold, Zhihong Cao,
378 and Erwin Klumpp. "Soil Organic Phosphorus Transformations During 2000 Years of Paddy-Rice and
379 Non-Paddy Management in the Yangtze River Delta, China." SCIENTIFIC REPORTS, 7 ,1-12.
380 <https://doi.org/10.1016/j.geoderma.2022.116296>.2017
- 381 Jiang, Xiaoqian, R Bol, S Willbold, H Vereecken, and E Klumpp. "Speciation and Distribution of P
382 Associated with Fe and Al Oxides in Aggregate-Sized Fraction of an Arable Soil." BIOGEOSCIENCES
383 12, no. 21 , 6443-52. <https://doi.org/10.5194/bg-12-6443-2015>.2015.
- 384 Jiang, Xiaoqian, Kenneth JT Livi, Mary R Arenberg, Ai Chen, Kai-yue Chen, Lowell Gentry, Zhe Li,
385 Suwei Xu, and Yuji Arai. "High Flow Event Induced the Subsurface Transport of Particulate Phosphorus
386 and Its Speciation in Agricultural Tile Drainage System." CHEMOSPHERE 263 , 128147.
387 <https://doi.org/10.1016/j.chemosphere.2020.128147>.2021
- 388 Jin, Yi, Xinqiang Liang, Miaomiao He, Yu Liu, Guangming Tian, and Jiyan Shi. "Manure Biochar
389 Influence Upon Soil Properties, Phosphorus Distribution and Phosphatase Activities: A Microcosm
390 Incubation Study."CHEMOSPHERE,142,12844<https://doi.org/10.1016/j.chemosphere.2015.07.015>.
391 2016
- 392 Jorgensen, PR, and Johnny Fredericia. "Migration of Nutrients, Pesticides and Heavy Metals in
393 Fractured." GEOTECHNIQUE, 42, no. 1 ,67-77. [https://doi.org/10.1016/0148-9062\(92\)91738-](https://doi.org/10.1016/0148-9062(92)91738-g)
394 [g](https://doi.org/10.1016/0148-9062(92)91738-g).1992.
- 395 Juma, NG, and MA Tabatabai. "Effects of Trace Elements on Phosphatase Activity in Soils."
396 SOILSCIENCE SOCIETY OF AMERICA JOURNAL,41,343-
397 46<https://doi.org/10.2136/sssaj1977.03615995004100020034x>.1977
- 398 Juma, NG, and MA Tabatabai "Phosphatase Activity in Corn and Soybean Roots: Conditions for Assay



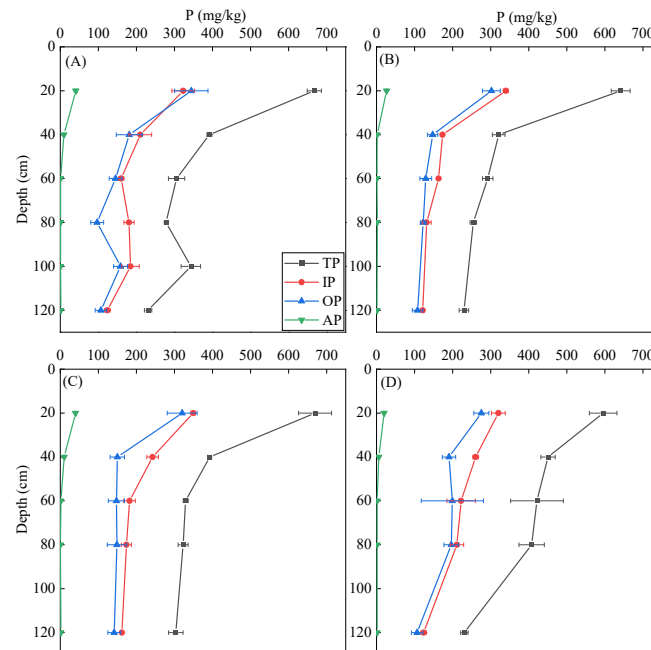
- 399 and Effects of Metals." *PLANT SOIL*, 107, no. 1 (1988): 39-47.
- 400 Kleber, M, R Mikutta, MS Torn, and R Jahn. "Poorly Crystalline Mineral Phases Protect Organic Matter
401 in Acid Subsoil Horizons." *EUROPEAN JOURNAL OF SOIL SCIENCE*, 56, 717-25.
402 <https://doi.org/10.1016/j.geoderma.2004.12.018>, 2005
- 403 Koopmans, GF, WJ Chardon, J Dolfing, O Oenema, P Van der Meer, and WH Van Riemsdijk. "Wet
404 Chemical and Phosphorus-31 Nuclear Magnetic Resonance Analysis of Phosphorus Speciation in a
405 Sandy Soil Receiving Long-Term Fertilizer or Animal Manure Applications." *JOURNAL OF*
406 *ENVIRONMENTAL QUALITY*, 32, no. 1, 287-95. <https://doi.org/10.2134/jeq2003.0287>, 2003
- 407 Koukol, Ondřej, Blanka Beňová, Magda Vosmanská, Tomáš Frantik, Miroslav Vosátka, and Marcela
408 Kovářová. "Decomposition of Spruce Litter Needles of Different Quality by *Setulipes Androsaceus* and
409 *Thysanophora Penicillioides*." *PLANT SOIL* 311, no. 1, 151-59. [https://doi.org/10.1007/s11104-008-](https://doi.org/10.1007/s11104-008-9666-5)
410 [9666-5](https://doi.org/10.1007/s11104-008-9666-5), 2008.
- 411 Krämer, Susanne, and Douglas M Green. "Acid and Alkaline Phosphatase Dynamics and Their
412 Relationship to Soil Microclimate in a Semiarid Woodland." *SOIL BIOLOGY/BIOCHEMISTRY*, 32, no.
413 2, 179-88. [https://doi.org/10.1016/S0038-0717\(99\)00140-6](https://doi.org/10.1016/S0038-0717(99)00140-6), 2000
- 414 Kronvang, B., R. Grant, and A. L. Laubel. "Sediment and Phosphorus Export from a Lowland Catchment:
415 Quantification of Sources." [In English]. *WATER AIR AND SOIL POLLUTION* 99, no. 1-4, 465-
416 76, 1997
- 417 Kronvang, Brian, Anker Laubel, and Ruth Grant. "Suspended Sediment and Particulate Phosphorus
418 Transport and Delivery Pathways in an Arable Catchment, Gelbaek Stream, Denmark."
419 *HYDROLOGICAL PROCESSES*, 11, no. 6 (1997): 627-42.
- 420 Li, Haigang, Jian Liu, Guohua Li, Jianbo Shen, Lars Bergström, and Fusuo Zhang. "Past, Present, and
421 Future Use of Phosphorus in Chinese Agriculture and Its Influence on Phosphorus Losses." *AMBIO*, 44,
422 274-85. <https://doi.org/10.1007/s13280-015-0633-0>, 2015
- 423 Li, Ying, Kenneth JT Livi, Mary R Arenberg, Suwei Xu, and Yuji Arai. "Depth Sequence Distribution of
424 Water Extractable Colloidal Phosphorus and Its Phosphorus Speciation in Intensively Managed
425 Agricultural Soils." *CHEMOSPHERE* 286, 131665.
426 <https://doi.org/10.1016/j.chemosphere.2021.131665>, 2022
- 427 Li, Ying, Kenneth JT Livi, Mary R Arenberg, Suwei Xu, and Yuji Arai. "Depth
428 Sequence Distribution of Water Extractable Colloidal Phosphorus and Its Phosphorus Speciation in
429 Intensively Managed Agricultural Soils." *CHEMOSPHERE*, 286, 131665.
430 <https://doi.org/10.1016/j.chemosphere.2021.131665>, 2022
- 431 Liang, Xinqiang, Yi Jin, Yue Zhao, Zhibo Wang, Rongqiang Yin, and Guangming Tian. "Release and
432 Migration of Colloidal Phosphorus from a Typical Agricultural Field under Long-Term Phosphorus
433 Fertilization in Southeastern China." *JOURNAL OF SOILS SEDIMENTS*, 16, 842-53.
434 <https://doi.org/10.1007/s11368-015-1290-4>, 2016
- 435 Liu, Jin, Barbara J Cade-Menun, Jianjun Yang, Yongfeng Hu, Corey W Liu, Julien Tremblay, Kerry
436 LaForge, et al. "Long-Term Land Use Affects Phosphorus Speciation and the Composition of Phosphorus
437 Cycling Genes in Agricultural Soils." *FRONTIERS IN MICROBIOLOGY*, 9, 1643.
438 <https://doi.org/10.3389/fmicb.2018.01643>, 2018
- 439 Masiello, CA, OA Chadwick, J Southon, MS Torn, and JW Harden. "Weathering Controls on
440 Mechanisms of Carbon Storage in Grassland Soils." *GLOBAL BIOGEOCHEMICAL CYCLES*, 18,
441 <https://doi.org/10.1029/2004GB002219>, 2004
- 442 McDowell, RW, I Stewart, and BJ Cade-Menun. "An Examination of Spin-Lattice Relaxation Times



- 443 for Analysis of Soil and Manure Extracts by Liquid State Phosphorus-31 Nuclear Magnetic Resonance
444 Spectroscopy." JOURNAL OF ENVIRONMENTAL QUALITY 35,293-302.
445 <https://doi.org/10.2134/jeq2005.0285.2006>
- 446 Murphy, JAMES, and John P Riley. "A Modified Single Solution Method for the Determination of
447 Phosphate in Natural Waters." ANALYTICA CHIMICA ACTA, 27, 31-36.
448 [https://doi.org/10.1016/s0003-2670\(00\)88444-5](https://doi.org/10.1016/s0003-2670(00)88444-5).1962.
- 449 Neubauer, Elisabeth, Walter DC Schenkeveld, Kelly L Plathe, Christian Rentenberger, Frank Von Der
450 Kammer, Stephan M Kraemer, and Thilo Hofmann. "The Influence of Ph on Iron Speciation in Podzol
451 Extracts: Iron Complexes with Natural Organic Matter, and Iron Mineral Nanoparticles." SCIENCE OF
452 THE TOTAL ENVIRONMENT 461, 108-16. <https://doi.org/10.1016/j.scitotenv.2013.04.076>. 2013.
- 453 Pote, DH, TC Daniel, PA Moore Jr, DJ Nichols, AN Sharpely, and DR Edwards. "Relating Extractable
454 Soil Phosphorus to Phosphorus Losses in Runoff." Soil Science Society of America Journal60, no. 3 ,
455 855-59. <https://doi.org/10.2136/sssaj1996.03615995006000030025x>.1996..
- 456 Rick, Allison R, and Yuji J Soil Science Society of America Journal Arai. "Role of Natural Nanoparticles
457 in Phosphorus Transport Processes in Ultisols." ,75,335-47.
458 <https://doi.org/10.2136/sssaj2010.0124nps>.2011.
- 459 Royer, Todd V, Mark B David, and Lowell E Gentry. "Timing of Riverine Export of Nitrate and
460 Phosphorus from Agricultural Watersheds in Illinois: Implications for Reducing Nutrient Loading to the
461 Mississippi River." ENVIRONMENTAL SCIENCE TECHNOLOGY,40,4126-31.
462 <https://doi.org/10.1021/es052573n>.2006.
- 463 Sanyal, SK, and SK De Datta. "Chemistry of Phosphorus Transformations in Soil." In Advances in Soil
464 Science, 1-120: Springer, 1991.
- 465 Séquaris, J-M, H %J Colloids Lewandowski, Surfaces A: Physicochemical, and Engineering Aspects.
466 "Physicochemical Characterization of Potential Colloids from Agricultural Topsoils." 217,93-99.
467 [https://doi.org/10.1016/S0927-7757\(02\)00563-0](https://doi.org/10.1016/S0927-7757(02)00563-0).2003.
- 468 Shanshan, Bai, TAN Jinfang, Zeyuan ZHANG, WEI Mi, Huimin ZHANG, and Xiaoqian JIANG.
469 "Phosphorus Speciation and Colloidal Phosphorus Response to the Cessation of Fertilization in Lime
470 Concretion Black Soil." PEDOSPHERE, <https://doi.org/10.1016/j.pedsph.2023.01.004> .2023.
- 471 Tabatabai, M Ali, and John M Bremner. "Use of P-Nitrophenyl Phosphate for Assay of Soil Phosphatase
472 Activity." SOIL BIOLOGY BIOCHEMISTRY 1, 301-07. [https://doi.org/10.1016/0038-0717\(69\)90012-1](https://doi.org/10.1016/0038-0717(69)90012-1).1969
- 473
- 474 Van Lierop, W "Determination of Available Phosphorus in Acid and Calcareous Soils with the
475 Kelowna Multiple-Element Extractant." SOILSCIENCE, 146,284 <https://doi.org/10.1097/00010694-198810000-00009>.1988.
- 476
- 477 Wang, Liming, Anna Missong, Wulf Amelung, Sabine Willbold, Jörg Prietzel, and Erwin Klumpp.
478 "Dissolved and Colloidal Phosphorus Affect P Cycling in Calcareous Forest Soils." GEODERMA
479 375 , 114507. <https://doi.org/10.1016/j.geoderma.2020.114507>.2020
- 480 Westermann, DT "Lime Effects on Phosphorus Availability in a Calcareous Soil." Soil Science SOCIETY
481 OF AMERICA JOURNAL 56, 489-94.
482 <https://doi.org/10.2136/sssaj1992.03615995005600020024x>.1992
- 483 Whalen, Joann K, and Chi Chang. "Phosphorus Accumulation in Cultivated Soils from Long-Term
484 Annual Applications of Cattle Feedlot Manure." Journal of environmental quality 30, 229-37.
485 <https://doi.org/10.2134/jeq2001.301229x>.2001
- 486 Williams, Mark R, Kevin W King, William Ford, Anthony R Buda, and Casey D Kennedy. "Effect of



487 Tillage on Macropore Flow and Phosphorus Transport to Tile Drains." WATER RESOURCES
488 RESEARCH, 52, 2868-82. <https://doi.org/10.1002/2015WR017650>.2016
489 WRB, Iwg. World Reference Base for Soil Resources 2014: International Soil Classification System for
490 Naming Soils and Creating Legends for Soil Maps. World Reference Base for Soil Resources 2014:
491 international soil classification system for naming soils and creating legends for soil maps, 2014.
492 Xue, Yuan, Mark B David, Lowell E Gentry, and David A Kovacic. "Kinetics and Modeling of Dissolved
493 Phosphorus Export from a Tile-Drained Agricultural Watershed." WILEY ONLINE LIBRARY, .
494 <http://doi/10.2134/jeq1999.00472425002800030048x>.1998.
495 Young, Eric O, Donald S Ross, Barbara J Cade-Menun, and Corey W Liu. "Phosphorus Speciation in
496 Riparian Soils: A Phosphorus-31 Nuclear Magnetic Resonance Spectroscopy and Enzyme Hydrolysis
497 Study." SOIL SCIENCE SOCIETY OF AMERICA JOURNAL,77,1636-47.
498 <https://doi.org/10.2136/sssaj2012.0313>.2013.
499 Zhao, Fengyan, Yongyong Zhang, Feike A Dijkstra, Zhijun Li, Yueqi Zhang, Tianshi Zhang, Yingqi Lu,
500 Jinwei Shi, and Lijuan Yang. "Effects of Amendments on Phosphorous Status in Soils with Different
501 Phosphorous Levels." CATENA,172,97-103. <https://doi.org/10.1016/j.catena.2018.08.016>.2019.
502
503
504
505
506
507
508
509
510
511
512
513
514
515
516
517
518
519



520

521 Fig. 1. The concentrations of available phosphorus (AP), total phosphorus (TP), inorganic phosphorus (IP), and

522 organic phosphorus (OP) in soil profiles of sample A, B, C, and D.

523

524

525

526

527

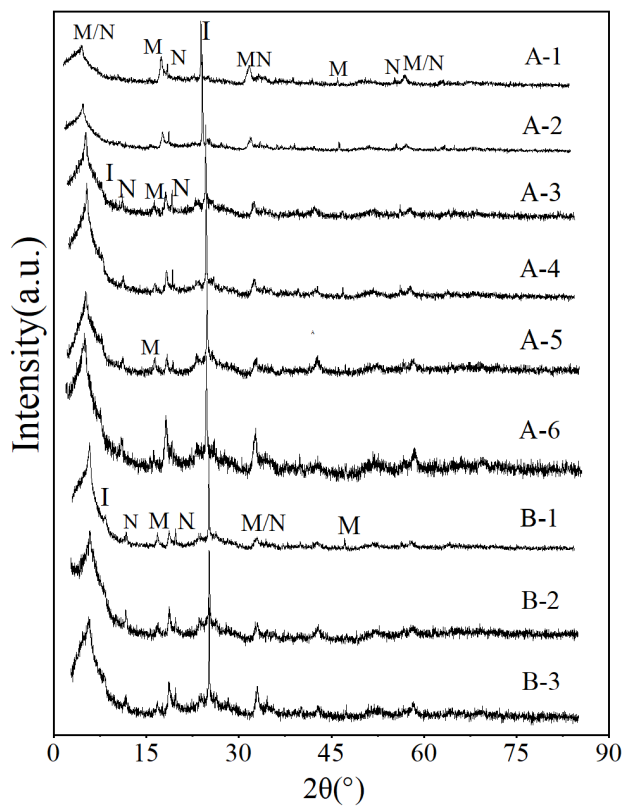
528

529

530

531

532



533

534 Fig. 2. XRD patterns of water-extractable colloid (WEC) fractions for soil sample A and B with different depths

535 (N: nontronite; M: montmorillonite; I: illite).

536

537

538

539

540

541

542

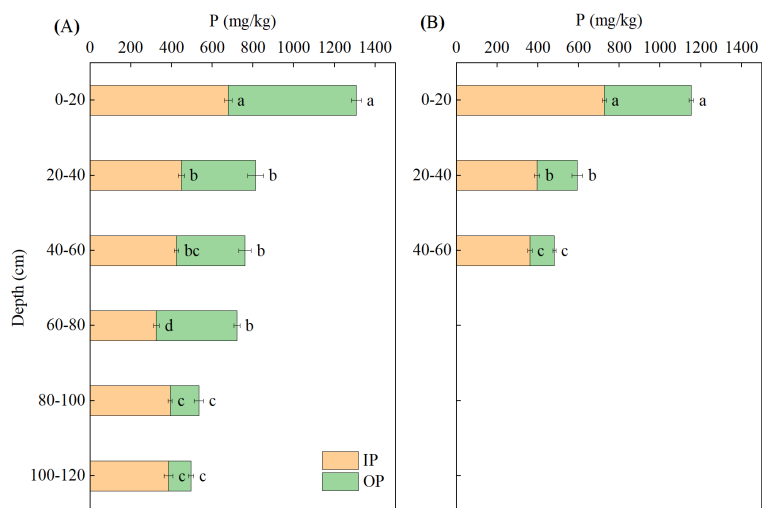
543

544

545

546

547



548

549 Fig.3 Inorganic (IP) and organic P (OP) concentrations (mg P/kg colloids) for water-extractable colloid (WEC)

550 fractions of sample A and B with different depths.

551

552

553

554

555

556

557

558

559

560

561

562

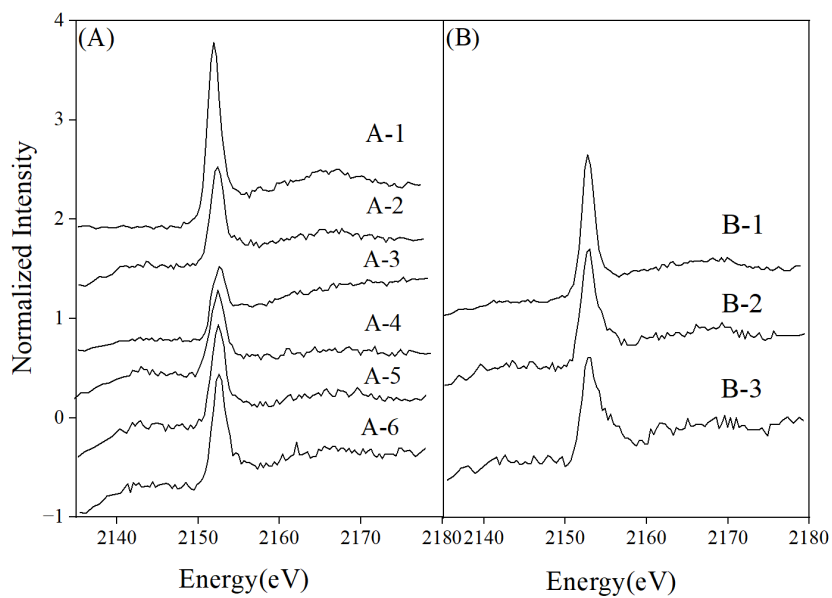
563

564

565

566

567



568
569 Figure 4. Linear combination fitting of P - K-edge XANES Spectra of water-extractable colloid (WEC) fractions
570 from profile soil (Samples A-1 to A-6 and B-1 to B-3).

571

572

573

574

575

576

577

578

579

580

581

582

583

584



585
586
587
588
589
590
591
592
593
594
595
596
597
598
599
600
601
602
603
604
605
606
607
608
609
610
611
612
613
614
615
616
617
618
619
620
621
622
623
624

Table 1 Physicochemical characteristics of bulk soils.

Sample	Depth(cm)	pH	%TC	%TN	C/P	ACP ($\mu\text{g}/(\text{g}^*\text{h})$)	ALP ($\mu\text{g}/(\text{g}^*\text{h})$)	OA-P (mg/kg)	DCB-P (mg/kg)
A	0-20	5.13±0.04e	0.91±0.00a	0.10±0.00a	15.3±0.9bc	647.8±13.5a	465.5±10.2a	142.9±0.8a	178.3±12.3a
	20-40	6.43±0.10d	0.54±0.01d	0.07±0.01b	12.1±0.6c	280.5±4.1b	305.3±14.1d	121.4±5.5b	121.4±5.5bc
	40-60	7.23±0.02c	0.52±0.00e	0.06±0.01bc	12.6±2.1c	213.3±6.7c	358.6±4.9c	137.6±6.5b	137.6±6.2b
	60-80	7.52±0.02b	0.67±0.01c	0.06±0.01bc	16.4±1.2b	127.8±9.8d	390.3±8.1b	31.9±3.5c	98.8±22.1c
	80-100	7.52±0.02b	0.75±0.01b	0.07±0.00b	22.1±1.9a	122.6±11.7d	414.0±11.1b	67.0±6.2b	103.1±16.7bc
B	100-120	7.70±0.02a	0.50±0.01f	0.06±0.01c	22.0±1.1a	96.2±8.2e	346.4±16.6c	75.8±15.3b	100.6±5.5c
	0-20	4.88±0.07e	1.17±0.01a	0.14±0.00a	17.5±1.2a	997.2±14.6a	701.4±14.7a	141.70±9.5a	185.9±2.8a
	20-40	6.28±0.02d	0.66±0.01b	0.08±0.00b	17.0±0.1a	413.0±4.7b	514.7±5.8b	84.7±1.3b	121.4±7.8b
	40-60	7.41±0.01c	0.48±0.00d	0.06±0.00c	14.6±0.3b	186.6±3.8c	509.3±17.9c	59.7±12.7c	66.6±11.4d
	60-80	8.03±0.01b	0.35±0.01e	0.05±0.00d	10.8±0.59c	147.2±14.3d	392.5±16.6d	73.7±3.2bc	99.8±2.8c
C	80-120	8.37±0.01a	0.52±0.01c	0.04±0.00c	17.2±0.4c	100.1±9.3e	326.2±14.3c	60.7±1.9c	79.1±0.9d
	0-20	5.01±0.02c	0.94±0.00a	0.11±0.00a	14.1±0.4b	1177.6±31.8a	510.6±15.2b	161.7±5.6a	182.3±6.0a
	20-40	6.23±0.03d	0.54±0.00b	0.07±0.00b	13.8±0.2b	332.4±12.8b	377.3±15.3d	33.7±0.7b	70.4±3.90b
	40-60	7.32±0.04c	0.48±0.00c	0.06±0.00c	16.4±1.1a	190.0±4.7c	578.1±7.6a	29.7±13.4b	45.6±8.8c
	60-80	7.60±0.03b	0.39±0.01d	0.04±0.01d	13.9±0.2b	176.6±3.2c	489.5±4.2b	41.7±6.2b	43.8±5.3c
D	80-120	7.74±0.03a	0.27±0.00e	0.04±0.00d	9.5±0.4c	126.8±17.9d	448.1±7.4c	48.7±4.81b	50.1±4.3c
	0-20	5.17±0.04e	0.88±0.01a	0.10±0.01a	13.8±0.4b	749.6±9.6a	502.1±12.9bc	126.7±6.2a	129.2±6.30a
	20-40	6.97±0.06d	0.57±0.02b	0.07±0.00b	18.0±0.3a	435.4±3.2b	557.2±14.6a	33.7±2.7b	51.4±2.07c
	40-60	7.46±0.03c	0.50±0.00c	0.06±0.00c	17.6±0.9a	136.7±5.8c	526.0±16.3b	34.7±7.0b	65.6±2.28b
	60-80	7.78±0.03b	0.36±0.01d	0.04±0.01cd	14.3±0.7b	175.9±6.5d	497.1±1.7c	42.7±5.7b	49.8±49.1c
	80-120	8.04±0.01a	0.25±0.00c	0.03±0.01d	10.9±0.6c	97.9±2.3e	349.4±10.3d	37.7±1.7b	40.1±1.93c



625

Table 2 Soil fractionation, physicochemical characteristics and P levels of water extracted colloids.

626

627

628

629

630

631

632

633

634

635

Sample	Depth (cm)	Soil texture	Soil sand fractions (>20 µm, %)	Soil silt fractions (2-20 µm, %)	Colloidal fraction (0.35-2 µm, %)	Zeta potential (mV)	Colloidal P (0.35-2 µm) (mg/kg soil)	DTP (<0.35µm, mg/kg soil)	DRP (<0.35µm, mg/kg soil)
A	0-20	sandy loam	57.0±4.0ab	34.8±3.8ab	6.2±0.3c	-19.1±2.7	80.7±3.6a	22.1±1.0a	10.0±1.3a
	20-40	sandy loam	55.7±1.4ab	34.2±1.2ab	6.3±0.3bc	-18.5±1.1	51.0±1.7b	15.3±0.9b	7.4±0.4b
	40-60	sandy loam	57.3±4.5	33.6±4.4ab	6.9±0.2bc	-17.9±0.6	52.4±1.9b	12.3±1.2c	4.6±1.1c
			ab						
	60-80	sandy loam	56.8±2.7ab	33.0±2.5ab	7.3±0.6ab	-17.5±2.9	52.9±4.4b	6.7±1.4d	2.6±0.5cd
B	80-100	sandy loam	59.7±2.9 a	30.4±3.3b	7.0±0.5bc	-15.7±2.7	37.3±1.3c	6.0±0.3d	2.0±0.7d
	100-120	loam	50.3±1.6 b	38.8±0.9a	8.3±0.5a	-15.8±0.8	41.2±1.4c	4.1±0.8d	1.2±0.3d
	0-20	sandy loam	56.3±3.4a	35.9±3.6a	5.3±0.3b	-22.0±1.7	61.3±2.7a	19.5±1.1a	10.0±1.3a
B	20-40	sandy loam	56.5±3.2a	34.8±4.1a	5.3±0.4b	-18.9±1.0	31.6±1.5b	14.4±1.2b	6.3±0.4b
	40-60	sandy loam	57.0±1.9a	33.1±1.2a	6.5±0.3a	-9.0±0.6	31.1±1.1b	11.2±0.9c	4.6±0.3b

636

DTP: total P concentrations of dissolved fractions (<0.35 µm); DRP: reactive P concentrations of dissolved fractions

637

(<0.35 µm).

638

639

640

641

642

643

644

645

646

647

648

649

650

651

652

653

654

655



656 Table 3. Concentrations of inorganic and organic P extracted by NaOH-Na₂EDTA (mg /kg⁻¹) in the
 657 water-extractable colloid (WEC) fractions of sample A and B by solution ³¹P-NMR.

Sample	Depth(cm)	Inorganic P (mg/kg)		Organic P (mg/kg)					
		Orth	Pyro	Orthophosphate Monoesters				Orthophosphate Diesters	
				Monoesters*	Myo-IHP	Scyllo-IHP	Other Monoesters	Diesters*	Glyc+nucl
A-1	0-20	202.4	10.1	50.6	8.1	3.5	39	89.1	81.0
A-2	20-40	46.8	5.1	62.0	1.4	0.0	60.6	15.4	1.8
A-3	40-60	14.1	0.14	42.2	0.6	2.0	39.6	11.4	0
A-4	60-80	14.0	0.84	38.5	0.4	0.00	38.1	0.0	0
A-5	80-100	15.3	5.5	39.6	9.2	0.00	30.4	8.1	3.5
A-6	100-120	12.5	0.0	36.3	3.8	0.00	32.5	7.5	3.8
B-1	0-20	427.5	8.6	128.3	4.3	17.6	106.4	21.4	8.5
B-2	20-40	121.0	7.3	128.1	3.7	0.00	124.4	12.2	7.3
B-3	40-60	57.5	10.4	52.9	3.5	0.00	49.4	1.7	1.7

661
662
663
664
665
666
667
668
669
670
671
672
673
674
675
676
677
678
679
680
681
682
683
684
685



686 Table 4 Phosphorus K-edge XANES fitting results showing the relative percent of each P species in
687 water-extractable colloid (WEC) fractions (%) of sample A and B.

688

Sample	Depth (cm)	Al-P (%)	Fe-P (%)	HAP (%)	IHP (%)
A-1	0-20	17.0±4.0	33.0±3.0a	10.0±2.0c	32.0±6.0a
A-2	20-40	13.0±2.0	30.0±5.0a	26.0±4.0bc	30.0±0.8ab
A-3	40-60	14.0±7.0	28.0±0.8a	32.0±7.0abc	26.0±5.0abc
A-4	60-80	12.0±1.0	29.0±3.0a	35.0±3.0abc	22.0±7.0abc
A-5	80-100	11.0±3.0	24.0±3.0ab	45.0±2.0ab	10.0±0.8c
A-6	100-120	9.0±7.0	16.0±3.0b	53.0±7.0a	13.0±5.0bc
B-1	0-20	25.0±7.0a	36.0±2.0a	13.0±3.0b	17.0±6.0
B-2	20-40	11.0±0.9b	19.0±6.0a	32.0±4.0ab	9.0±4.0
B-3	40-60	3.0±0.6b	20.0±5.0b	60.0±10.0a	7.0±4.0

696 Al-P: aluminum phosphate (AlPO_4), Fe-P: iron phosphate dihydrate ($\text{FePO}_4 \cdot 2\text{H}_2\text{O}$), HAP:
697 hydroxyapatite ($\text{Ca}_5(\text{PO}_4)_3\text{OH}$), and IHP: inositol hexakisphosphate. Values in each column followed
698 by the different lowercase letters indicate significant differences ($P < 0.05$).

699
700
701